

## Steady-state and transient photolysis of p-nitroaniline in acetonitrile

Hongjuan Ma<sup>a,b</sup>, Side Yao<sup>a</sup>, Jing Zhang<sup>a,b</sup>, Changyong Pu<sup>a,b</sup>, Sufang Zhao<sup>a,b</sup>,  
Min Wang<sup>a,\*</sup>, Jie Xiong<sup>c</sup>

<sup>a</sup> Shanghai Institute of Applied Physics, Chinese Academy of Sciences, P.O. Box 800-204, Shanghai 201800, PR China

<sup>b</sup> Graduate School of Chinese Academy of Sciences, Beijing 100039, PR China

<sup>c</sup> Institute of Nuclear Physics and Chemistry, China Academy of Engineering Physics, Mianyang 621900, PR China

### ARTICLE INFO

#### Article history:

Received 15 August 2008  
Received in revised form  
10 November 2008  
Accepted 21 November 2008  
Available online 28 November 2008

#### Keywords:

p-Nitroaniline  
Photo-degradation  
Laser flash photolysis  
Excited state  
UV/H<sub>2</sub>O<sub>2</sub>

### ABSTRACT

Both transient photolysis and steady-state photo-degradation experiments were performed to gain insight into the kinetics and mechanisms of degradation of p-nitroaniline (p-NA) in acetonitrile (MeCN) solutions. Complete degradation of p-NA was observed at diverse irradiation conditions under 254 nm UV light. Once H<sub>2</sub>O<sub>2</sub> was added into the experimental system, degradation of p-NA was enhanced remarkably. The removal rate increased rapidly with increment of the irradiation time and reached 90% at 30 min. p-NA could be totally removed after 90 min in UV/H<sub>2</sub>O<sub>2</sub> process. In the presence of O<sub>2</sub> and H<sub>2</sub>O<sub>2</sub>, removal rate increased linearly with increment of the irradiation time and reached 90% at 10 min. p-NA could be totally removed after 20 min in UV/(O<sub>2</sub> + H<sub>2</sub>O<sub>2</sub>) process. For transient photolysis, excited states of p-NA were observed after 355 and 266 nm laser flash photolysis (LFP). The transient absorption spectra were recorded and bimolecular rate constant of  $6.89 \times 10^9 \text{ M}^{-1} \text{ s}^{-1}$  was calculated for the self-quenching of <sup>3</sup>p-NA\*. Production of <sup>3</sup>p-NA\* in MeCN and H<sub>2</sub>O mixed solution was also studied. LFP of p-NA with addition of H<sub>2</sub>O<sub>2</sub> was investigated for the first time.

© 2008 Elsevier B.V. All rights reserved.

### 1. Introduction

p-Nitroaniline (p-NA) is an important compound either manufactured or used as an intermediate such as in the synthesis of dyes, antioxidants, pharmaceuticals, gum inhibitors, poultry medicines, pesticides, etc. As a consequence, a plethora of p-NA is leaked out with industrial wastewater into the environment. Unfortunately, p-NA has been found to be harmful to aquatic organisms and may cause long-term damage to the environment. It is highly toxic with a TLV (threshold limit value) of  $0.001 \text{ kg m}^{-3}$ , which is lower than that of aniline ( $0.002 \text{ kg m}^{-3}$ ). The presence of a nitro group in the aromatic ring enhances its stability to resist chemical and biological oxidation degradation, while the anaerobic degradation produces nitroso and hydroxylamines compounds which are known as carcinogenic [1–3]. Nowadays, p-NA has been considered as one kind of persistent organic pollutants (POPs) due to its toxicity, potential carcinogenic and mutagenic effects, and treatments of p-NA containing wastewater have attracted world-wide attention [3–5].

In recent years, advanced oxidation processes (AOPs) have been identified as an attractive option for wastewater purification, particularly in cases where the contaminant species are difficult to be removed using biological or physicochemical processes. The

processes involve the generation of highly reactive hydroxyl radical (<sup>•</sup>OH), which can oxidize and mineralize almost all organic molecules owing to its high oxidation potential ( $E^\circ = +2.8 \text{ V}$ ) [6–8]. UV light or sunlight has been used in the direct photo-degradation of contaminants in aqueous environments, but neither is considered as an efficient method. Since the late 1960s, many studies have indicated that the UV/H<sub>2</sub>O<sub>2</sub> process is able to oxidize a wide variety of organic pollutants in aqueous solutions [9–11]. Generally, the effectiveness of homogeneous light-driven oxidation processes is associated with <sup>•</sup>OH radicals generated in the reaction mixture by the direct photolysis of an added component (e.g., H<sub>2</sub>O<sub>2</sub>) under UV irradiation.



The success of direct photolysis is highly dependent on the photo-reactivity of the organic compounds. Hence, the properties of the pollutants and the photo-degradation mechanism should be investigated beforehand because the degradation mechanism of organic substances is often complex, especially in diverse reaction conditions. Consequently, individual degradation systems must be designed to study the properties of target pollutants. Besides, some reactive intermediates might undergo further reactions and be present at undetectable concentrations. Hence, their transient existence can only be inferred from the kinetic data and/or other means. Laser flash photolysis (LFP) and pulse radiolysis techniques have been used to study the mechanism involved. The intersystem cross-

\* Corresponding author. Tel.: +86 2159554934.  
E-mail address: [wangm@sinap.ac.cn](mailto:wangm@sinap.ac.cn) (M. Wang).

ing (ISC), internal conversion, and vibrational relaxation of p-NA in water and 1,4-dioxane have been studied using ultrafast transient absorption spectroscopy. The data reveal that relaxation on the excited singlet state surface, followed by internal conversion to the ground-state and intersystem crossing to the triplet state [1]. In this paper, excited states of p-NA were studied in MeCN solution, whose polarity is higher than 1,4-dioxane and lower than water. Transient photolysis of p-NA in MeCN was investigated using 355 and 266 nm LFP. And photochemical properties of p-NA were studied. Furthermore, LFP of p-NA with  $\text{H}_2\text{O}_2$  was investigated for the first time. Early in the year 1977, Van Der Linde had determined the reaction rate constant of p-NA with  $\cdot\text{OH}$  using pulse radiolysis [12]. However, the data have never been used to associate with any practical degradation research. Although some researches such as photo-catalytic degradation has been done to understand the degradation mechanism [5], to the authors' knowledge, there is little information available in the literature about the detailed degradation mechanism of p-NA in MeCN solution, especially the cooperation of  $\cdot\text{OH}$  with  $\text{O}_2$ . In this study, both steady-state photodegradation and transient photolysis experiments of p-NA were performed to gain insight into the kinetics and mechanisms of photo-induced degradation of p-NA in MeCN. The main objectives of the present work are to elucidate the mechanisms of photo-induced degradation of p-NA and consequently to provide kinetic insight into utilization for remediation of p-NA-laden wastewaters.

## 2. Experimental

### 2.1. Chemical reagents

p-Nitroaniline, tert-butanol (t-BuOH) and 30%  $\text{H}_2\text{O}_2$  were of analytical grade purchased commercially. Acetonitrile (MeCN) was chromatographic purity grade.  $\text{O}_2$  and  $\text{N}_2$  gases were of high purity (99.99%). Other reagents were used directly without further purification. All solutions were fresh prepared using water from a Milli-Q purification system just before experiment.

### 2.2. Laser flash photolysis experiments

LFP experiments were performed with a ND:YAG laser which provided 266 and 355 nm pulses with a duration of 5 ns. The maximum laser power was 50 and 80 mJ/pulse, respectively. The samples for photolysis experiments were all bubbled with high-purity (99.99%)  $\text{N}_2$  or  $\text{N}_2\text{O}$  in quartz cuvettes for 20 min before use. The time-resolved experiments were all carried out at  $15 \pm 2^\circ\text{C}$ . The detailed description of the facility and experimental conditions can be found elsewhere [13,14].

### 2.3. Photo-degradation procedures and analysis

The irradiation source is hexagonal in cross section of 9 cm side length. Six low-pressure Hg lamps (8W), which emit 253.7 nm UV light, are arranged on each side of the device made of stainless steel and coated by aluminum foil for light reflection. Samples in quartz cuvettes were located in the center of the lamps. Details of the device can be referred to a Chinese Patent [15].

Concentrations of p-NA were determined by gas chromatography (Varian CP 3800) with a column (VF-5MS,  $30\text{ m} \times 0.25\text{ mm} \times 0.25\text{ }\mu\text{m}$ ). The column temperature was initially held at  $50^\circ\text{C}$  for 2 min and then programmed up to  $300^\circ\text{C}$  at  $20^\circ\text{C min}^{-1}$ . UV-vis absorption spectra were measured by a Hitachi UV-3010 spectrophotometer. All experiments were carried out at ambient temperatures ( $25 \pm 2^\circ\text{C}$ ).

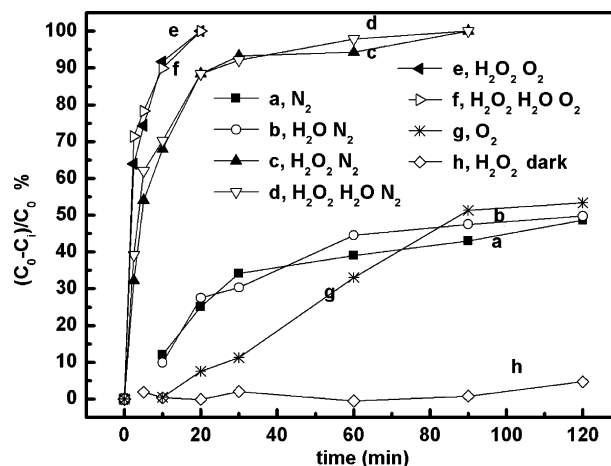


**Fig. 1.** Removal rates of 1 mM p-NA in MeCN solutions at different conditions: (a)  $\text{N}_2$  saturated; (b)  $\text{N}_2$  saturated with  $\text{H}_2\text{O}_2$ ; (c)  $\text{N}_2$  saturated with  $\text{H}_2\text{O}_2$  and  $\text{H}_2\text{O}$ ; (d)  $\text{N}_2$  saturated with  $\text{H}_2\text{O}_2$  and  $\text{H}_2\text{O}$ ; (e)  $\text{O}_2$  saturated with  $\text{H}_2\text{O}_2$ ; (f)  $\text{O}_2$  saturated with  $\text{H}_2\text{O}_2$  and  $\text{H}_2\text{O}$ ; (g)  $\text{O}_2$  saturated; (h) with  $\text{H}_2\text{O}_2$  in dark.

## 3. Results and discussion

### 3.1. Remove of p-NA in MeCN under 254 nm UV light

#### 3.1.1. Direct remove of p-NA in MeCN

Series of p-NA MeCN solutions were irradiated at 254 nm UV light; and the removal rate is shown in Fig. 1. In  $\text{N}_2$  saturated experimental system, removal rate increased slowly along with increment of the irradiation time and reached 50% after 120 min (Fig. 1a). When p-NA solution was saturated with  $\text{O}_2$ , removal rate was reduced slightly at the beginning of the irradiation but also reached 50% after 120 min (Fig. 1g). With the progress of photolysis the color of the solution became brownish gradually and precipitates were obtained.

The following content will expound that p-NA can be photo-excited directly to produce its excited states in  $\text{N}_2$  saturated MeCN solution. Then excited states of p-NA interact with its ground-state spontaneously to form dimers, trimers (Eqs. (2)–(4)), and eventually result in higher oligomers and polymers of low solubility, which can be easily separated from the solution. In  $\text{O}_2$  saturated experimental system, excited states of p-NA can be quenched by  $\text{O}_2$  to produce singlet oxygen ( $^1\text{O}_2^*$ ) (Eq. (5)). Accordingly, the yield of triplet states of p-NA ( $^3\text{p-NA}^*$ ) will be reduced. Hence, the removal rate was a little lower than that of  $\text{N}_2$  saturated experimental system at the very beginning of the irradiation. However,  $^1\text{O}_2^*$  is also one of the most oxidizing and reactive species. It is extensively involved in the degradation of organic pollutants as the result of its high oxidative activation ( $E^\circ = +2.2\text{ V}$ ). Obviously, both  $\text{N}_2$  and  $\text{O}_2$  experience the increase in color intensity and form precipitates during reaction, and they are both oxidation processes, which lead removal of p-NA in MeCN solution with lower rate.

#### 3.1.2. Effect of $\cdot\text{OH}$ and cooperation with $\text{O}_2$ in photo-degradation of p-NA

Once  $\text{H}_2\text{O}_2$  was added into the experimental system, removal rates of p-NA were enhanced remarkably. In  $\text{N}_2$  saturated solution with addition of 0.147 M  $\text{H}_2\text{O}_2$ , removal rate increased rapidly along with increment of the irradiation time and reached almost 90% in 30 min. p-NA could be totally degraded after 90 min (Fig. 1c and d). In order to rule out direct oxidative of  $\text{H}_2\text{O}_2$  in the photo-degradation process, p-NA solution with addition of 0.147 M  $\text{H}_2\text{O}_2$  was kept in dark. And p-NA could not be degraded (Fig. 1h). This means that  $\cdot\text{OH}$  generated from  $\text{H}_2\text{O}_2$  by 254 nm UV light-induced photo-degradation of p-NA in MeCN. The mechanism of  $\cdot\text{OH}$ -

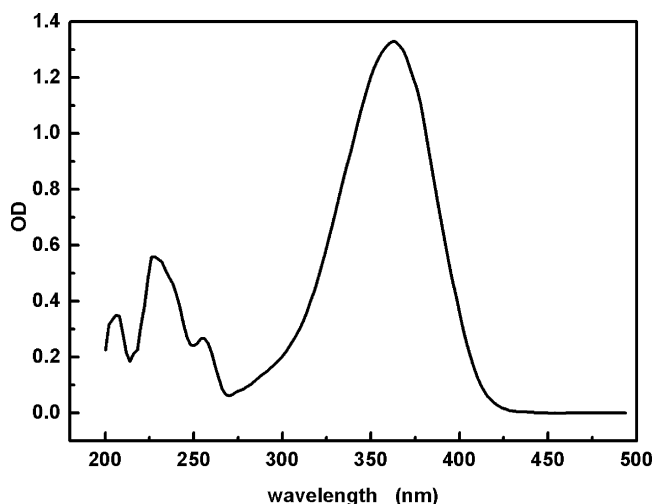


Fig. 2. UV-vis spectrum of 0.1 mM p-NA in MeCN solution.

induced degradation of p-NA has been discussed in earlier study, which suggested that  $\cdot\text{OH}$  was very efficient in the degradation of p-NA [12].

$\text{O}_2$  saturated solution with addition of  $\text{H}_2\text{O}_2$  resulted in the most efficient degradation of p-NA. Removal rate increased linearly along with increment of the irradiation time in 2.5 min and reached almost 90% in 10 min and p-NA could be totally degraded after 20 min (Fig. 1e and f). This means  $\text{O}_2$  played a crucial role in the degradation of p-NA when it cooperated with  $\cdot\text{OH}$ . It had been concluded in the literature about the mechanism. Peroxide is formed when  $\text{O}_2$  adds to the nitro substituted hydroxycyclohexadienyl radicals, which gives birth to the final ring cleavages [16,17]. In comparison with the following results, 10% of  $\text{H}_2\text{O}$  was added into the MeCN solution and no distinct difference was observed (Fig. 1b, d and f). This means the differences between photo-excitation and photo-ionization of p-NA in the degradation process can be ignored.

### 3.2. Photolysis of p-NA in MeCN with 355 nm LFP

#### 3.2.1. Studies of excited states of p-NA with 355 nm LFP

UV-vis spectrum of 0.1 mM p-NA in MeCN solution shows p-NA has strong absorption in the wavelength region of 330–400 nm (Fig. 2). This means 355 nm light can be well absorbed by p-NA. In order to get better transient spectra, the photolysis of p-NA was firstly performed in MeCN solutions with 355 nm LFP. Fig. 3 depicts the transient absorption spectra obtained from 355 nm LFP of  $\text{N}_2$  saturated 0.05 mM p-NA MeCN solution. The spectra recorded at 0.05 and 1.5  $\mu\text{s}$  after laser pulse were characterized by absorption bands with a maximum at 400 nm and a weaker one at 520 nm. The transient species with absorption at 400 and 520 nm decayed completely in less than 2  $\mu\text{s}$ . When the experimental system was saturated with  $\text{O}_2$ , the transient species at 400 and 520 nm were quenched (inset of Fig. 3). Hence, these two absorption bands might be assigned to  $^3\text{p-NA}^*$ . It has been found that the decay of  $^3\text{p-NA}^*$  at 400 nm increased with the increment of p-NA concentration in the range of 0.005–0.1 mM in  $\text{N}_2$  saturated solutions. This result indicated that  $^3\text{p-NA}^*$  underwent self-quenching and the decay of absorption at 400 nm followed a mono-exponential kinetics. From a plot of the pseudo-first-order rate constant of the triplet decay versus the ground-state concentration (Fig. 4), bimolecular rate constant of  $6.89 \times 10^9 \text{ M}^{-1} \text{ s}^{-1}$  was calculated for the self-quenching ( $k_{\text{sq}}$ ). From the intercept, monomolecular rate constant ( $k_0$ ) of  $2.28 \times 10^6 \text{ s}^{-1}$  represented self-decaying rate constant of  $^3\text{p-NA}^*$ . The same rate constant for the self-quenching obtained at

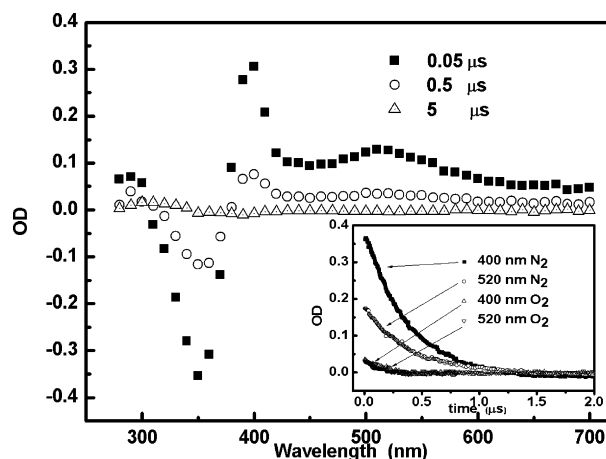


Fig. 3. Transient absorption spectra obtained from 355 nm LFP of  $\text{N}_2$  saturated 0.05 mM p-NA MeCN solution recorded at (■) 0.05  $\mu\text{s}$ ; (○) 0.5  $\mu\text{s}$ ; (△) 5  $\mu\text{s}$  after laser pulse. Inset: formation and decay traces of the transient absorption at 400 nm (■)  $\text{N}_2$  saturated; (△)  $\text{O}_2$  saturated and 520 nm (○)  $\text{N}_2$  saturated; (▽)  $\text{O}_2$  saturated from 355 nm LFP of  $\text{N}_2$  saturated 0.05 mM p-NA MeCN solution.

520 nm ( $6.57 \times 10^9 \text{ M}^{-1} \text{ s}^{-1}$ ) confirmed that the species with maximum at 520 nm also belong to  $^3\text{p-NA}^*$ .

So the mechanism of 355 nm LFP of p-NA can be illustrated as following: p-NA can be photo-excited directly by 355 nm LFP in MeCN solution to produce its excited singlet states ( $^1\text{p-NA}^*$ ) which then converts to its excited triplet states ( $^3\text{p-NA}^*$ ) following intersystem crossing process (Eq. (2)).  $^3\text{p-NA}^*$  can be quenched by ground-state of p-NA at the rate of  $6.89 \times 10^9 \text{ M}^{-1} \text{ s}^{-1}$  to form stable products such as dimers, trimers, and eventually result in higher oligomers and polymers (Eq. (4)). These oligomers and polymers induce intensity color and precipitates in the degradation process. Besides,  $^3\text{p-NA}^*$  can be quenched by  $\text{O}_2$  to produce singlet oxygen ( $^1\text{O}_2^*$ ) (Eq. (5)). The rate constants of  $^3\text{p-NA}^*$  quenched by  $\text{O}_2$  ( $k_q$ ) were determined to be  $9.8 \times 10^9 \text{ M}^{-1} \text{ s}^{-1}$ . Nevertheless,  $^1\text{O}_2^*$  may induce the oxidation of p-NA further [18,19].

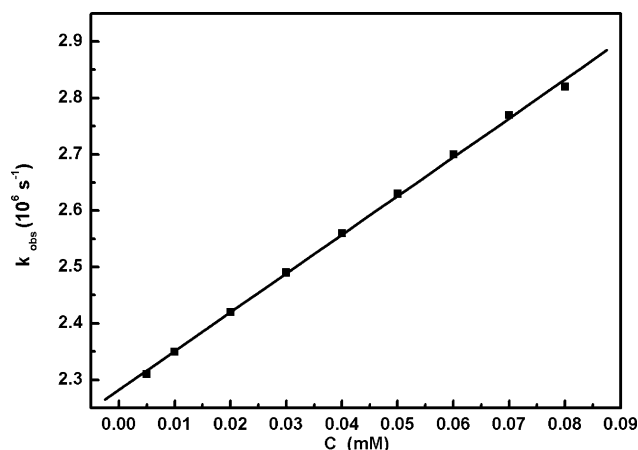
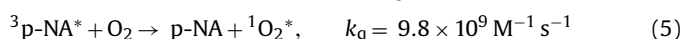
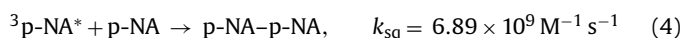
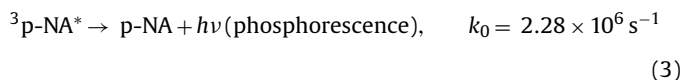
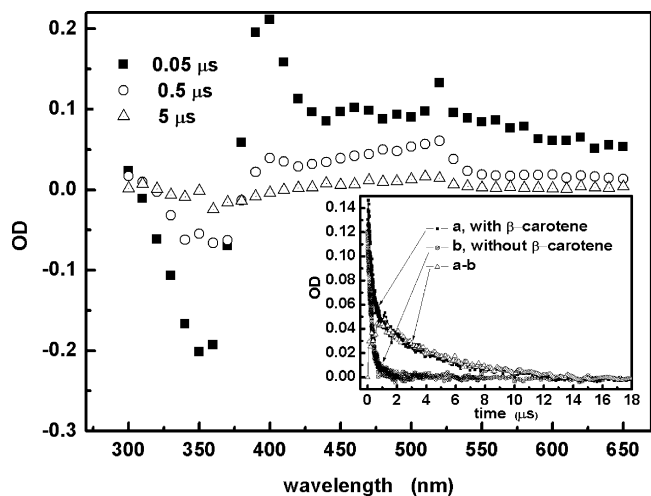


Fig. 4. The self-quenching rate constant for  $^3\text{p-NA}^*$  observed at 400 nm from 355 nm LFP was determined as  $6.89 \times 10^9 \text{ M}^{-1} \text{ s}^{-1}$ .



**Fig. 5.** Transient absorption spectra obtained from 355 nm LFP of  $N_2$  saturated 0.05 mM p-NA MeCN solution containing 0.02 mM  $\beta$ -carotene recorded at (■) 0.05  $\mu$ s; (○) 0.5  $\mu$ s; (△) 5  $\mu$ s after laser pulse. Inset: formation and decay traces of the transient absorption from 355 nm LFP of  $N_2$  saturated 0.05 mM p-NA MeCN solution at 520 nm (■) with  $\beta$ -carotene; (○) without  $\beta$ -carotene (△)  $^3\beta$ -C $^*$  by subtracting the absorbance of  $^3p$ -NA $^*$ .

### 3.2.2. Energy transfer from $^3p$ -NA $^*$ to $\beta$ -carotene ( $\beta$ -C)

To further identify  $^3p$ -NA $^*$ , the energy transfer between  $^3p$ -NA $^*$  and  $\beta$ -carotene was investigated. Photolysis of 0.02 mM  $\beta$ -carotene in MeCN solution by 355 nm LFP showed no transient absorption. Fig. 5 shows the transient absorption spectra recorded after the 355 nm LFP of  $N_2$  saturated 0.05 mM p-NA MeCN solution containing 0.02 mM  $\beta$ -carotene. At 0.5  $\mu$ s after the pulse, accompanying the decay of the absorption band in the wavelength region of 380–420 nm, a new absorption peak at 520 nm grew up. As shown in the inset of Fig. 5, an obvious formation process at 520 nm was observed by subtracting the absorbance of  $^3p$ -NA $^*$  at 400 nm. Here, the transient species with absorption peak at 520 nm could be assigned to  $^3\beta$ -carotene $^*$  according to the energy transfer from  $^3p$ -NA $^*$  (Eq. (6)) [20].



### 3.2.3. Studies of photo-ionization of p-NA with 355 nm LFP

The transient absorption spectra observed from 355 nm LFP of  $N_2$  saturated 0.05 mM p-NA MeCN solution also exhibited an absorption peak at 300 nm (Fig. 3). When the experimental system was saturated with  $O_2$ , intensity of the absorbance at 300 nm did not decrease. Hence, the peak at 300 nm might be radical cation ( $p\text{-NA}^{\bullet+}$ ) or neutral radical ( $p\text{-NA}^*$ ) or both of them from photo-ionization of p-NA. This indicated that p-NA could be not only photo-excited to produce its excited states but also be photo-ionized by 355 nm LFP in MeCN solution. Photo-ionization of p-NA would give birth to  $e_{\text{sol}}^-$  and  $p\text{-NA}^{\bullet+}$  (Eq. (7)). Hence, the peak at 300 nm was  $p\text{-NA}^{\bullet+}$  or  $p\text{-NA}^*$  via deprotonation (Eq. (8)) or both of them. Two neutral radicals can also interact spontaneously to form dimmers. This could be another reason why the color of the solution became brownish and precipitates were obtained. The transient species with maximum absorption over 680 nm, which could be assigned as  $e_{\text{sol}}^-$ , were not observed as  $e_{\text{sol}}^-$  was eliminated by MeCN (Eq. (9)).



At wavelengths shorter than 380 nm the transient absorption spectra exhibited a strong initial absorption bleaching (Fig. 3) reflecting that pump-induced ground-state depletion dominated the observed dynamics. As the concentration of bleached p-NA equals to the concentration of formed transient species, individual LFP system can be designed to study the proportion between photo-excitation and photo-ionization by comparing the transient absorption  $OD_0$  (optical density value recorded at 0 time after laser pulse).

$$OD_{0(\lambda=350N_2)} = \varepsilon(C_{\text{photo-excitation}} + C_{\text{photo-ionization}}) L = -0.2998 \quad (10)$$

$$OD_{0(\lambda=350O_2)} = \varepsilon(C_{\text{photo-ionization}}) L = -0.1968 \quad (11)$$

where  $OD_{0(\lambda=350N_2)}$  and  $OD_{0(\lambda=350O_2)}$  are  $OD_0$  values recorded at 350 nm in  $N_2$  and  $O_2$  saturated system, respectively (Fig. 6).  $C_{\text{photo-excitation}}$  and  $C_{\text{photo-ionization}}$  are the depletion of p-NA by photo-excitation and photo-ionization, respectively. In  $N_2$  saturated system,  $OD_0$  at 350 nm was larger than that of  $O_2$  saturated system. As a result, photo-ionization had a proportion of 65.64% and photo-excitation of 34.35% by 355 nm LFP in MeCN solution. This indicates that photo-ionization lead a dominant position in photolysis of p-NA.

Comparing the transient absorbance  $OD_0$  after laser pulse and at 350, 400 and 520 nm, molar extinction coefficients  $\varepsilon_{(\lambda=400 \text{ nm})}$ ,  $\varepsilon_{(\lambda=520 \text{ nm})}$  of  $^3p$ -NA $^*$  can be deduced via the following equalities as the concentration of bleached p-NA equals to the concentration of formed  $^3p$ -NA $^*$ .

$$OD_{\lambda=350 \text{ nm}} = \varepsilon_{\lambda=350 \text{ nm}} C_{\lambda=350 \text{ nm}} L \quad (12)$$

$$OD_{\lambda x} = \varepsilon_{\lambda x} C_{\lambda x} L \quad (13)$$

$$(12)/(13) \quad \varepsilon_{\lambda=350 \text{ nm}} OD_{\lambda x} = \varepsilon_{\lambda x} OD_{\lambda=350 \text{ nm}} \quad (14)$$

$$OD_{0(\lambda=350N_2)} - OD_{0(\lambda=350O_2)} = -0.2998 - (-0.1968) = -0.103$$

$$OD_{0(\lambda=400)} = 0.36276$$

$$OD_{0(\lambda=520)} = 0.17463$$

where  $\varepsilon_{\lambda=350 \text{ nm}}$  and  $OD_{\lambda=350 \text{ nm}}$  are the molar extinction coefficient and the OD value of transient species recorded at wavelength of 350 nm after the pulse, and  $\varepsilon_{\lambda x}$ ,  $OD_{\lambda x}$  at the certain wavelength. The  $\varepsilon_{\lambda=350 \text{ nm}}$  of p-NA is determined as  $12,870 \text{ M}^{-1} \text{ cm}^{-1}$  in MeCN solution. Hence, the molar extinction coefficients  $\varepsilon_{\lambda=400 \text{ nm}}$  and  $\varepsilon_{\lambda=520 \text{ nm}}$  of  $^3p$ -NA $^*$  can be obtained to be  $45,327$  and  $21,820 \text{ M}^{-1} \text{ cm}^{-1}$ , respectively.

### 3.3. Studies of excited states of p-NA in MeCN and $H_2O$ mixed solution with 355 nm LFP

$H_2O$  will come along inevitably with 30%  $H_2O_2$  added in the steady-state photo-degradation experiments. Hence, photolysis of p-NA in MeCN and  $H_2O$  mixed solution with 355 nm LFP was also performed by ultrafast transient absorption spectroscopy. The formation and decay traces of  $^3p$ -NA $^*$  recorded at 400 nm in diverse systems were investigated.  $OD_0$  values at 400 nm decreased with the increase of amount of  $H_2O$  added into the solution. And lifetime of  $^3p$ -NA $^*$  recorded at 400 nm was shortened distinctly. When the amount of  $H_2O$  exceeded 10%, even no  $^3p$ -NA $^*$  was observed. Synchronously, with the addition of water, in a very short time at 0.05  $\mu$ s after the pulse a strong absorption appeared in a broad wave-length region of 480–800 nm. The strong, broad range of 580–800 nm disappeared when system was saturated with  $N_2O$

**Table 1**  
Proportions of photo-excitation and photo-ionization in MeCN/H<sub>2</sub>O mixed solution.

Ratio of H <sub>2</sub> O (v/v) (%)	OD <sub>0(λ=400)</sub>	Ratio of photo-excitation (%)	Ratio of photo-ionization (%)
0	0.34522	34.35	65.64
5	0.24818	24.96	75.04
10	0.00142	0.14	99.86
50	0	0	100
100	0	0	100

with the addition of t-BuOH. Hence, the transient species with maximum absorption around 680 nm could be assigned as e<sub>aq</sub><sup>-</sup>. This means p-NA was directly photo-ionized. Proportion of photo-excitation in each system can be calculated likewise and the result is shown in Table 1.

Time-resolved microwave conductivity measurements suggest that the quantum yield for ISC of p-NA in benzene is close to 100%, whereas a reduced quantum yield of about 50% is observed for p-NA in the slightly more polar dioxane. This indicates that even small changes in the solvent polarity have a big impact on the quantum yield of <sup>3</sup>p-NA\*. This suggests that dissolving p-NA in a very polar solvent, such as water, may result in a very small quantum yield [21]. With the addition of 0.147 M H<sub>2</sub>O<sub>2</sub> in steady-state photo-degradation experiments, about 1.17% H<sub>2</sub>O was added into the system, both photo-excitation and photo-ionization took place (Table 1). And the removal rate is shown in Fig. 1c and e. When 10% of H<sub>2</sub>O was added into the steady-state photo-degradation system, no distinct difference was observed (Fig. 1d and f). In this condition, photo-ionization led a very dominant position in photolysis of p-NA and photo-excitation could be ignored. This means in the •OH-induced degradation process, different functions of excited states and ionized states of p-NA might be ignored.

### 3.4. Photolysis of p-NA in MeCN with 266 nm LFP

#### 3.4.1. Studies of excited states of p-NA in MeCN with 266 nm LFP

The studies of triplet states of p-NA were also performed in MeCN solutions with 266 nm LFP in accord with the steady-state photolysis experiments. The transient absorption spectra obtained did not basically differ from that of 355 nm LFP except that bleaching could not be observed as penetrability of light of 266 nm is weaker than that of 355 nm (Fig. 3 and Fig. 7). The decay traces of the transient absorption at 400 and 520 nm under 266 nm LFP were consistent with that of 355 nm LFP. They decayed completely in less than 2 μs in N<sub>2</sub> saturated MeCN solution. When the experimental system was saturated with O<sub>2</sub>, the transient species observed at 400

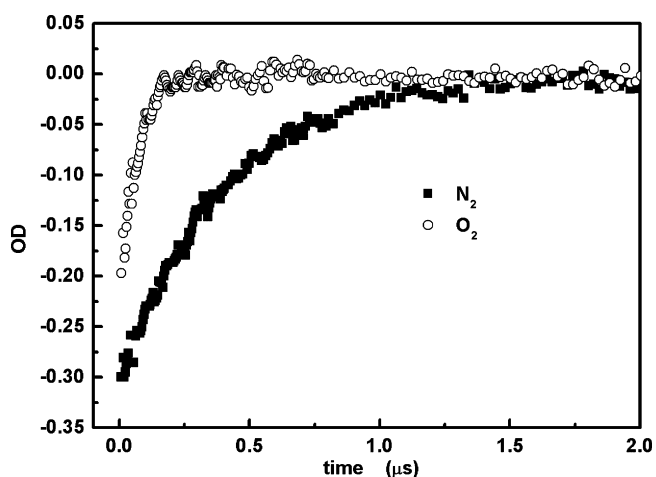


Fig. 6. Formation and decay traces at 350 nm (■) N<sub>2</sub> saturated; (○) O<sub>2</sub> saturated.

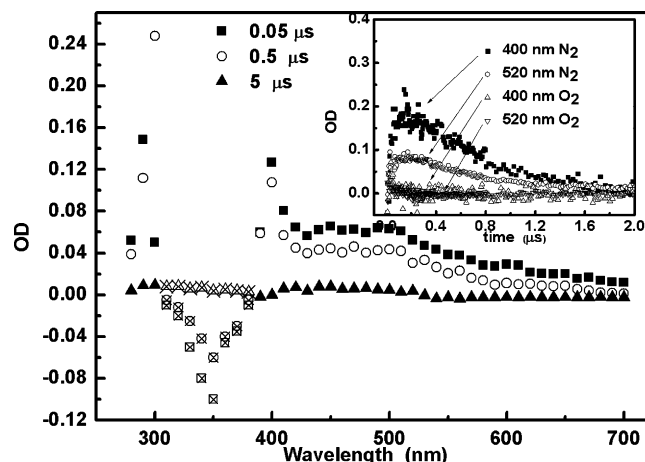


Fig. 7. Transient absorption spectra obtained from 266 nm LFP of N<sub>2</sub> saturated 0.1 mM p-NA MeCN solution at (■) 0.05 μs; (○) 0.5 μs; (▲) 5 μs after 266 nm LFP. (Bleachings in the range of 320–380 nm were open marked as they cannot be observed after 266 nm LFP in this experimental system.) Insert: formation and decay traces of the transient absorption at 400 nm (■) N<sub>2</sub> saturated; (△) O<sub>2</sub> saturated and 520 nm (○) N<sub>2</sub> saturated; (▽) O<sub>2</sub> saturated from 266 nm LFP of N<sub>2</sub> saturated 0.1 mM p-NA MeCN solution.

and 520 nm were quenched (insert Fig. 7). Hence, these two absorption bands could also be assigned as <sup>3</sup>p-NA\*. This meant that p-NA could also be photo-excited directly by 266 nm LFP in MeCN (Eq. (15)). The absorption peak at 300 nm suggested that p-NA could be directly photo-ionized by 266 nm light in MeCN (Eq. (16)). However, the proportion between photo-excitation and photo-ionization was not obtained as bleaching could not be observed.



#### 3.4.2. Studies of excited states of p-NA with addition of H<sub>2</sub>O<sub>2</sub> in MeCN under 266 nm LFP

H<sub>2</sub>O<sub>2</sub> is weakly absorbing compounds in the UV range, and the absorption increases as the wavelength decreases. For example, at λ = 254 and 266 nm, the molar absorption coefficients ε is 21.2 and 10.7 M<sup>-1</sup> cm<sup>-1</sup>, respectively. For p-NA at λ = 254 and 266 nm, ε is 2670 and 860 M<sup>-1</sup> cm<sup>-1</sup>, respectively. H<sub>2</sub>O<sub>2</sub> can absorb the [10.7 × 22 / (10.7 × 22 + 860 × 0.1)] × 100% = 73% of 266 nm photons and p-NA can absorb 27% 266 nm photons. Hence, in dilute MeCN solutions of 0.1 mM p-NA in the presence of 0.022 M H<sub>2</sub>O<sub>2</sub>, both H<sub>2</sub>O<sub>2</sub> and p-NA are principal absorber of UV light. The transient absorption spectra recorded after the 266 nm LFP of N<sub>2</sub> saturated 0.1 mM p-NA and 0.022 M H<sub>2</sub>O<sub>2</sub> MeCN solutions are shown in Fig. 8b. Meanwhile, equivalent amount of H<sub>2</sub>O was added in MeCN solutions to make a comparison (Fig. 8a). The transient absorption spectra were similar with each other at the first 0.5 μs. Transient species with absorption at 400 nm could also be assigned as <sup>3</sup>p-NA\*. However, an absorption band with a maximum at 450 nm was recorded at 5 μs after laser pulse with the addition of H<sub>2</sub>O<sub>2</sub> (Fig. 8b). The formation and decay traces of the transient absorption at 450 nm in each system are shown in Fig. 9. The growth trace of transient species in pure H<sub>2</sub>O<sub>2</sub> system at 450 nm was obtained with the method of subtraction [22]. The lifetime of this transient species is about 10 μs with a formation process in 2.5 μs. Kinetic analyses showed that the growth trace followed the first order kinetics well. These transient species probably belong to the reaction of p-NA with •OH which came from the photo-decomposition of H<sub>2</sub>O<sub>2</sub>.

The photolysis of H<sub>2</sub>O<sub>2</sub> in pure water has been studied extensively by various groups of researchers in the 1950s [23–27] in order to elucidate the reaction mechanism. The general consensus

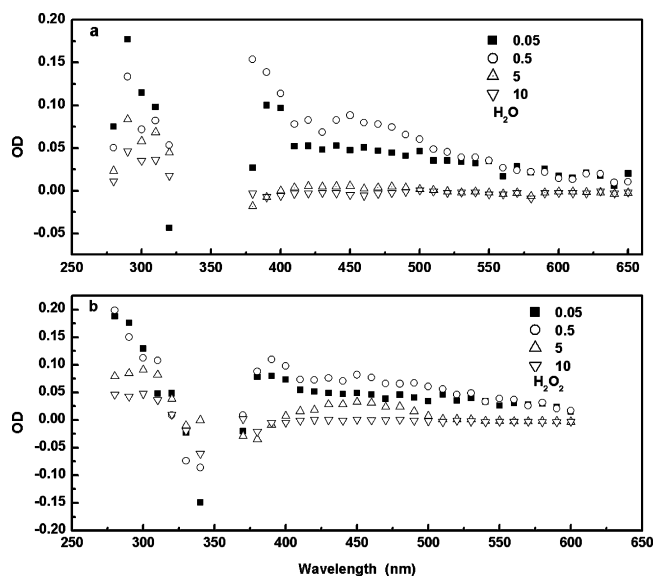
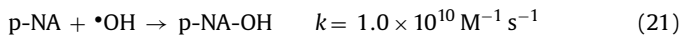
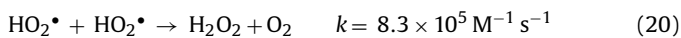
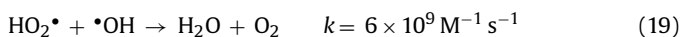
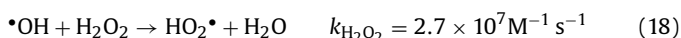


**Fig. 8.** Transient absorption spectra obtained from 266 nm LFP of  $N_2$  saturated 0.1 mM p-NA MeCN solution with (a) 0.25%  $H_2O$  and (b) 0.022 M  $H_2O_2$  at (■) 0.05  $\mu s$ ; (○) 0.5  $\mu s$ ; (△) 5  $\mu s$ ; (▽) 10  $\mu s$  after the 266 nm laser pulse.

of the reaction scheme below describes  $H_2O_2$  photo-decomposition in pure water (Eqs. (17)–(20)):



Thus, photo-decomposition  $H_2O_2$  generates the very highly oxidizing and reactive radical  $\bullet OH$ . Transient reaction of p-NA with  $\bullet OH$  was studied using pulse radiolysis. The transient absorption spectra after the pulse radiolysis of  $N_2O$  saturated p-NA aqueous solution were recorded and the reaction rate constant were determined as  $1.0 \times 10^{10} M^{-1} s^{-1}$  (Eq. (21)) [12]. This indicated that  $\bullet OH$  could react with p-NA at a rate near the diffusion-controlled limit. The mechanism of  $\bullet OH$ -induced degradation of p-NA has been discussed in earlier

study, which suggested that  $\bullet OH$  played the main role in the degradation of p-NA. Generally,  $\bullet OH$  radical is considered to be very reactive, and the addition reactions of  $\bullet OH$  are associated with very low barriers, and essentially unselective reactivity [28]. When  $\bullet OH$  initially added to the aromatic ring of p-NA, series of  $\bullet OH$  adducts came into being, which resulted in the complete degradation of p-NA (Fig. 1c and d). In the presence of  $O_2$ , peroxide was formed when  $O_2$  added to the nitro substituted hydroxylcyclohexadienyl radicals. Most of the ring cleavages came from these peroxide compounds producing alcohols, aldehydes and acids [16,17,29–32]. That is the reason why  $O_2$  saturated with addition of  $H_2O_2$  exhibited the highest removal rate in Fig. 1e and f.

#### 4. Conclusions

LFP is an efficient technique to study the properties of the pollutants and the photo-degradation mechanism involved. p-NA can be photo-excited and photo-ionized by 355 and 266 nm LFP in MeCN solution. Energy transfer between  ${}^3p\text{-NA}^*$  and  $\beta$ -carotene was investigated to identify  ${}^3p\text{-NA}^*$ . The transient absorption spectra were recorded and bimolecular rate constant of  $6.89 \times 10^9 M^{-1} s^{-1}$  was calculated for the self-quenching of  ${}^3p\text{-NA}^*$ . Proportion between photo-excitation and photo-ionization was obtained after 355 nm LFP. And photo-ionization leads a dominant position in photolysis of p-NA. Production of  ${}^3p\text{-NA}^*$  in MeCN and  $H_2O$  mixed solution was also investigated. And the reaction of p-NA with  $\bullet OH$  which comes from the photo-decomposition of  $H_2O_2$  was obtained from 266 nm LFP for the first time. For steady-state photo-degradation, the removal rate of p-NA is in the order of  $UV/(O_2 + H_2O_2) > UV/H_2O_2 > UV$ . It means that radical reactions played an important role in the photo-degradation process. The removal of p-NA by  $\bullet OH$  is much more efficient than direct oxidation by 254 nm light. When  $O_2$  cooperates with  $\bullet OH$ , degradation efficient was much more remarkable. Based on the results of the above, it can be concluded that the sequential use of  $H_2O_2$  and  $O_2$  has remarkable advantage in the treatment of p-NA-containing wastewaters.

#### Acknowledgement

This work was financially supported by the National Natural Science Foundation of China (Grant No. 10676036).

#### References

- [1] C.L. Thomsen, J. Thøgersen, S.R. Keiding, Ultrafast charge-transfer dynamics: studies of p-nitroaniline in water and dioxane, *J. Phys. Chem. A* 102 (1998) 1062–1067.
- [2] M.A. Oturan, J. Peiroten, P. Chartrin, A.J. Acher, Complete destruction of p-nitrophenol in aqueous medium by electro-Fenton method, *Environ. Sci. Technol.* 34 (2000) 3474–3479.
- [3] A. Saupe, High-rate biodegradation of 3- and 4-nitroaniline, *Chemosphere* 39 (1999) 2325–2346.
- [4] J.H. Sun, S.P. Sun, M.H. Fan, H.Q. Guo, L.P. Qiao, R.X. Sun, A kinetic study on the degradation of p-nitroaniline by Fenton oxidation process, *J. Hazard. Mater.* 148 (2007) 172–177.
- [5] G. Satyen, P.K. Sanjay, B.S. Sudhir, G. Vishwas, Pangarkar, Photocatalytic degradation of 4-nitroaniline using solar and artificial UV radiation, *Chem. Eng. J.* 110 (2005) 129–137.
- [6] C.P. Huang, C. Dong, Z. Tang, Advanced chemical oxidation: its present role and potential future in hazardous waste treatment, *Waste Manage.* 13 (1993) 361–377.
- [7] R. Andreozzi, V. Caprio, A. Insola, R. Marotta, Advanced oxidation processes (AOP) for water purification and recovery, *Catal. Today* 53 (1999) 51–59.
- [8] E. Neyens, J. Baeyens, A review of classic Fenton's peroxidation as an advanced oxidation technique, *J. Hazard. Mater.* 98 (2003) 33–50.
- [9] M. Saquib, M. Abu Tariq, M.M. Haque, M. Muneer, Photocatalytic degradation of disperse blue 1 using UV/TiO<sub>2</sub>/H<sub>2</sub>O<sub>2</sub> process, *J. Environ. Manage.* 88 (2008) 300–306.
- [10] Y.L. Nie, C. Hu, J.H. Qu, X.X. Hu, Efficient photodegradation of Acid Red B by immobilized ferrocene in the presence of UVA and H<sub>2</sub>O<sub>2</sub>, *J. Hazard. Mater.* 154 (2008) 146–152.

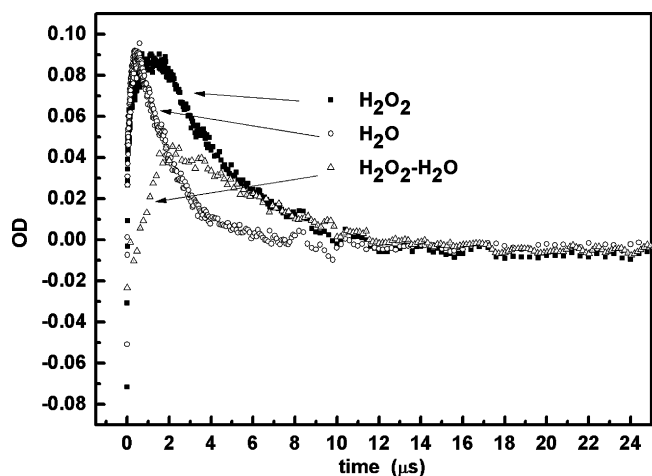


**Fig. 9.** Formation and decay traces of the transient absorption at 450 nm obtained from 266 nm LFP of  $N_2$  saturated 0.1 mM p-NA MeCN solution (■) with  $H_2O_2$ ; (○) with  $H_2O$ ; (△)  $H_2O_2$  subtract from  $H_2O$ .

- [11] J. Dwyer, L. Kavanagh, P. Lant, The degradation of dissolved organic nitrogen associated with melanoidin using a UV/H<sub>2</sub>O<sub>2</sub> AOP, *Chemosphere* 71 (2008) 1745–1753.
- [12] H.J. Van Der Linde, A pulse radiolytic study of aqueous nitroaniline solutions, *Radiat. Phys. Chem.* 10 (1977) 199–206.
- [13] H.P. Zhu, Z.X. Zhang, H.W. Zhao, W.F. Wang, S.D. Yao, Transient species and its properties of melatonin, *Sci. Chin. B: Chem.* 49 (2006) 308–314.
- [14] D.Y. Dou, Y.B. Liu, H.W. Zhao, L. Kong, S.D. Yao, Radiolysis and photolysis studies on active transient species of diethylstilbestrol, *J. Photochem. Photobiol. A: Chem.* 171 (2005) 209–214.
- [15] S.D. Yao, D.M. Xu, D.Y. Dou, H.W. Sun, K.L. Sheng, J.H. Yu, J. Hong, Polymer experiment equipment. Chinese Patent 200,520,042,466.4 (2006).
- [16] H.J. Ma, M. Wang, R.Y. Yang, W.F. Wang, J. Zhao, Z.Q. Shen, S.D. Yao, Radiation degradation of Congo Red in aqueous solution, *Chemosphere* 68 (2007) 1098–1104.
- [17] I. Loeff, G. Stein, The radiation and photochemistry of aqueous solutions of benzene, *J. Chem. Soc.* (1963) 2623–2633.
- [18] M.A. Gondal, H.M. Masoudi, J. Pola, Laser photo-oxidative degradation of 4,6-dimethyldibenzothiophene, *Chemosphere* 71 (2008) 1765–1768.
- [19] M.J. Zhan, X. Yang, Q.M. Xian, L.R. Kong, Photosensitized degradation of bisphenol A involving reactive oxygen species in the presence of humic substances, *Chemosphere* 63 (2006) 378–386.
- [20] G.L. Zhu, G.Z. Wu, D.W. Long, M.L. Sha, S.D. Yao, Laser photolysis of ionic liquid [bmim][PF<sub>6</sub>], *Nucl. Sci. Technol.* 18 (2007) 16–19.
- [21] W. Schuddeboom, J.M. Warman, H.A.M. Biemans, E.W. Meijler, Dipolar triplet states of p-nitroaniline and N-alkyl derivatives with one-, two-, and three-fold symmetry, *J. Phys. Chem.* 100 (1996) 12369–12373.
- [22] H.P. Zhu, H.W. Zhao, Z.X. Zhang, W.F. Wang, S.D. Yao, Laser flash photolysis study on antioxidant properties of hydroxycinnamic acid derivatives, *Radiat. Environ. Biophys.* 45 (2006) 73–77.
- [23] J.H. Baxendale, J.A. Wilson, The photolysis of hydrogen peroxide at high light intensities, *Trans. Faraday Soc.* 53 (1957) 344–356.
- [24] J.L. Weeks, M.S. Matheson, The primary quantum yield of hydrogen peroxide decomposition 1, *J. Am. Chem. Soc.* 78 (1956) 1273–1278.
- [25] J.P. Hunt, H. Taube, The photochemical decomposition of hydrogen peroxide. quantum yields, tracer and fractionation effects, *J. Am. Chem. Soc.* 74 (1952) 5999–6002.
- [26] F.S. Dainton, J. Rowbottom, The primary radical yield in water. A comparison of the photolysis and radiolysis of solutions of hydrogen peroxide, *Trans. Faraday Soc.* 49 (1953) 1160–1173.
- [27] K. Li, M.I. Stefan, J.C. Crittenden, Trichloroethene degradation by UV/H<sub>2</sub>O<sub>2</sub> advanced oxidation process: product study and kinetic modeling, *Environ. Sci. Technol.* 41 (2007) 1696–1703.
- [28] A. Grand, C. Morell, V. Labet, J. Cadet, L.A. Eriksson, •H atom and •OH radical reactions with 5-methylcytosine, *J. Phys. Chem. A* 111 (2007) 8968–8972.
- [29] C. Bouquet-Somrani, A. Finiels, P. Graffin, J.L. Olive, Photocatalytic degradation of hydroxylated biphenyl compounds, *Appl. Catal. B* 8 (1996) 101–106.
- [30] K. Hashimoto, T. Kawai, T. Sakata, Photocatalytic reactions of hydrocarbons and fossil fuels with water. Hydrogen production and oxidation, *J. Phys. Chem.* 88 (1984) 4083–4088.
- [31] L. Cermenati, P. Pichat, C. Guillard, A. Albini, Probing the TiO<sub>2</sub> photocatalytic mechanisms in water purification by use of Quinoline, photo-Fenton generated •OH radicals and superoxide dismutase, *J. Phys. Chem. B* 101 (1997) 2650–2658.
- [32] X. Li, J.W. Cabbage, W.S. Jenks, Photocatalytic degradation of 4-chlorophenol 2. The 4-chlorocatechol pathway, *J. Org. Chem.* 64 (1999) 8525–8536.